


Geophysical Research Letters[®]



RESEARCH LETTER

10.1029/2023GL106854

Fault Kinematic Modeling Along a Widely Deformed Plate Boundary in Southern Italy

Marco Cuffaro¹ , Patrizio Petricca², Alessia Conti¹, Mimmo Palano^{1,3} , Andrea Billi¹ , and Sabina Bigi⁴

¹Cnr-Istituto di Geologia Ambientale e Geoingegneria, Rome, Italy, ²ISPRA–Servizio Geologico d'Italia, Rome, Italy,

³Istituto Nazionale di Geofisica e Vulcanologia, Osservatorio Etneo, sezione di Catania, Catania, Italy, ⁴Dipartimento di Scienze della Terra, Sapienza Università di Roma, Rome, Italy

Key Points:

- We combine 392 recent Global navigation satellite system rates and the geometry of 160 faults of southern Italy to compute new strain rate field using numerical methods
- We present fault kinematics of the region and compare it to reference literature
- We obtain a tectonic setting which suggests this approach is useful to investigate fault kinematics along diffuse plate boundaries

Supporting Information:

Supporting Information may be found in the online version of this article.

Correspondence to:

M. Cuffaro,
marco.cuffaro@igag.cnr.it

Citation:

Cuffaro, M., Petricca, P., Conti, A., Palano, M., Billi, A., & Bigi, S. (2024). Fault kinematic modeling along a widely deformed plate boundary in southern Italy. *Geophysical Research Letters*, *51*, e2023GL106854. <https://doi.org/10.1029/2023GL106854>

Received 16 OCT 2023
Accepted 22 DEC 2023

Abstract Convergent plate boundaries are often characterized by widely deformed zones, where coexisting tectonic processes and variable fault kinematics can occur. Here, we quantify this variability along the Africa-Eurasia deformed boundary in southern Italy, based on the evaluation of geodetic strain rate by recent space geodesy observations and plate motions, which are integrated by main geometric properties of detected faults in the area. We propose a compilation of 160 known faults. We use numerical methods to predict fault kinematics and net slip rate, due to the geodetic deformation field with the inclusion of fault strain accommodation. The obtained tectonic setting is compared with the observable, showing a fault rake agreement of the 73%, which allows us to consider this approach potentially favorable to improve the knowledge of fault kinematics along diffuse plate boundaries, when fault properties are not directly available.

Plain Language Summary A boundary between two plates is not a single line but it is often a large area with diffuse deformation, simultaneous tectonic processes and complex geodynamics. Here, we analyze the Africa-Eurasia convergent and deformed boundary in southern Italy, central Mediterranean, where the lineaments along which crustal blocks move, the faults, show variable motion directions. We integrated the data describing the accurate displacement of the Earth's surface coming from recent satellite observations and from global plate motion models, together with geometric characteristics of 160 known faults, which we compiled for the purpose of computing the deformation field, that is, the geodetic strain rate, and kinematics along the faults of the area, using numerical methods. The procedure to integrate geodetic and geological observed data allows us to model crustal deformation both offshore and onshore the study area, and the agreement of the 73% between observed versus predicted fault kinematics suggests that this approach can help to investigate tectonics deformation along diffuse plate boundaries worldwide, when fault properties cannot be directly observed.

1. Introduction

Plate boundaries are rarely defined by a single interface. Indeed, they often comprise diffuse deformation zones, illuminated by topography and bathymetry, seismicity, and fault distribution (Bird, 2003; Gordon & Stein, 1992; Kreemer et al., 2014). Convergent margins, in particular, are characterized by widely deformed zones and large orogenic belts, such as along the Nazca-South America plate boundary or between the Eurasia plate and the Africa, Anatolia, Arabia and India plates, where the size of the related orogens and the deformation zones, that is, the Andes and the Alpine-Himalayas system, generally grows proportionally with increasing convergent plate kinematics (Allmendinger et al., 2007; Cuffaro & Doglioni, 2018; Motaghi et al., 2017; Xiao & Santosh, 2014). In those tectonic settings, morphology described by topography and bathymetry show a variability of fault direction and kinematics, which is a consequence of changes in strain and stress accommodation or by the coexistence of different tectonic processes (Allmendinger et al., 2005; Cuffaro et al., 2011; Guillaume et al., 2022, and references therein).

Southern Italy is located within the deformed Africa (AF)–Eurasia (EU) plate boundary in the central Mediterranean Sea, where the magnitude of the geodetic strain rate derived by the global strain rate model GSRM v.2.1 (Kreemer et al., 2014) is around 60–80 nstrain/a. Convergence between plates (Figure 1) is accommodated by compression along the southern Tyrrhenian Sea, extension between Sicily and Calabria (Kreemer et al., 2014; Palano et al., 2015, 2017), complex active tectonics in the Sicily Channel (Civile et al., 2021; Corti et al., 2006; Palano et al., 2020) and by a variable geodynamic setting in the Ionian Sea due to the Calabrian Arc subduction

© 2024. The Authors.

This is an open access article under the terms of the [Creative Commons Attribution License](https://creativecommons.org/licenses/by/4.0/), which permits use, distribution and reproduction in any medium, provided the original work is properly cited.

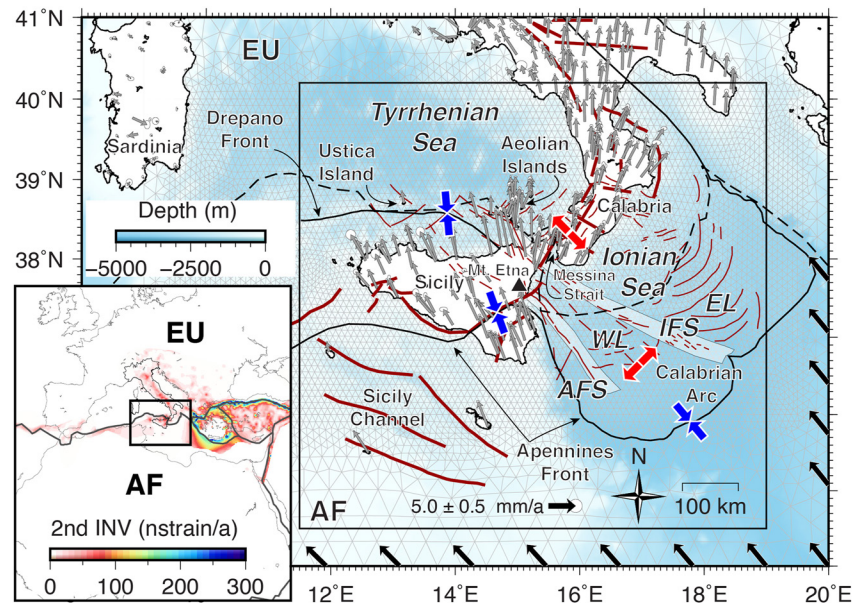


Figure 1. Tectonic settings in southern Italy and 2-D computation grid. Brown lines are the compiled fault lineaments derived from the Database of Individual Seismogenic Sources (DISS) database (thick lines, with associated slip rate, DISS Working Group, 2021), and additional literature (thin lines, with no slip rate, e.g., Billi et al., 2007; Polonia et al., 2016). Solid and dashed black lines are the compression fronts and the Eurasia (EU)–Africa (AF) plate boundary from DeMets et al. (2010). Shaded areas are the Ionian Fault System (IFS) and the Alfeo-Etna Fault System (AFS). Gray and black vectors are the Global navigation satellite system velocities after Billi et al. (2023) and the computed rates relative to fixed EU, respectively. Blue and red arrows denote compression and extension areas. In the lower left inset, the second invariant of the GSRM v.2.1 geodetic strain rate model by Kreemer et al. (2014) is reported, and the solid black lines are plate boundaries from DeMets et al. (2010). EL–Eastern Lobe, WL–Western Lobe.

(Gutscher et al., 2016; Polonia et al., 2016). Observed data in this latter sector are derived by marine geology acquisitions, and complexity is characterized by combination of the compression due to plate motions and trans-tensional tectonics along the Alfeo-Etna Fault and the Ionian Fault Systems (Gutscher et al., 2016; Polonia et al., 2016; Presti, 2020; Proietti et al., 2021; Sgroi et al., 2021). The latter separates the accretionary prism in the Western Lobe and the Eastern Lobe. There, seismically active faults are observed (Figure 1). Distribution of faults and their kinematics in southern Italy are described by morphological interpretation of topography and bathymetry (Billi et al., 2007; Gutscher et al., 2016; Monaco et al., 2002), seismic reflection profiles (Bortoluzzi et al., 2017; Gallais et al., 2013; Polonia et al., 2016, 2017), seismicity (Presti, 2020; Totaro et al., 2016), and paleoseismology (Galli & Peronace, 2015).

Space geodesy helps to characterize the areas of tectonic compression and extension (Cuffaro et al., 2011; Kreemer et al., 2014; Palano et al., 2015). In those cases, geodetic strain rate computed by Global Navigation Satellite System (GNSS) velocities does not consider the location and geometry of faults in numerical solutions.

In this paper, we compute a new geodetic strain rate field, fault slip rates and net slip rates in southern Italy, integrating GNSS velocities, global plate motions and available geologic data on fault geometry. We tested this approach by adopting numerical methods with the NeoKinema code (Bird & Liu, 2007), which computes long-term-average anelastic strain rate, derived fault kinematics and fault offset rates. To this scope, we compiled 160 fault lineaments as well as a recent geodetic velocity field. Our main aim is (a) to increase the grid resolution (5 km) of the numerical solutions along the short segment of the AF-EU boundary and (b) to predict tectonic setting in southern Italy with the integration of geodetic and geologic record, comparing results with observable.

2. Data and Methods

Our approach consists of evaluating regional-to-local geodetic crustal deformation with the inclusion of fault properties within our study area. It is based on the analysis and processing of the available data following three main steps: (a) compilation of the traces of active faults with any available rakes and/or offset rates; (b) collection

of a dense list of GNSS stations with location coordinates and local velocity components; (c) use of the code NeoKinema v5.4 (Bird & Liu, 2007) to model faults and continuum deformation of the study area.

(i) In southern Italy, we compiled 160 digitalized fault traces located in 12 sectors which are the Southern Tyrrhenian Faults (STF), the Southern Tyrrhenian Transcurrency (STT), the Sicily Onland Transcurrency (SOT), the Ionian Fault System (IFS), the Western Lobe Faults (WLF), the Alfeo-Etna Fault System (AFS), the Calabria Offshore Faults (COF), the Eastern Lobe Compression (ELC), the Western Lobe Compression (WLC), the Calabria-Sicily Faults (CSF), the Southern Tyrrhenian Extension (STE) and the Gioia Basin Faults (GBF), plus two compression fronts (i.e., the Drepano and the Apennines fronts), which characterize the active deformation in the study area (Figures 1–3 and in Supporting Information S1). We merged data sets mainly from Billi et al. (2007), Carminati et al. (2010), Polonia et al. (2016), and Doglioni et al. (2012) with auxiliary information by existing literature (Figures S1–S5 in Supporting Information S1). An additional sector is the Database of Individual Seismogenic Sources (DISS) (DISS Working Group, 2021), but we did not include the sources in southern Tyrrhenian and Ionian Sea to avoid overlaps of crustal deformation results with faults used in Billi et al. (2007) and Polonia et al. (2016). Fault offset rate components are described by the primary and secondary slip, that is, the dominant and the minor sense of the offset for a specific fault. They are not largely available and were constrained as initial condition only for the DISS database (Table S1 in Supporting Information S1). All compiled fault properties are reported in Table S1 in Supporting Information S1.

(ii) A recent GNSS velocity field in the ITRF14 reference frame (Altamimi et al., 2017) was obtained by Billi et al. (2023). We integrated that solution computing additional GNSS rates spanning the 1995.00–2023.00 time period, and extending the field westward to Sardinia and northward to the 42°N parallel (Figure 1), to include more continuous GNSS stations. To neglect local velocity outliers (e.g., Hammond et al., 2016; Jiang et al., 2022; Pan et al., 2021), we removed from the final solution all sites biased by large velocity uncertainties and/or showing suspicious movements with respect to nearby sites (~0.2% of the data set here analyzed). For example, stations close to Mt. Etna were not considered to avoid the short-term volcanic deformation signature (Palano et al., 2022). The velocity field can be considered as an interseismic solution, since no large earthquakes ($M > 6$) occurred in the study area during the measurement time-window. A final database of 392 GNSS velocities is provided (Figure 1 and Table S2 in Supporting Information S1), using processing methodologies adopted in Billi et al. (2023).

(iii) We modeled data obtained in (i) and (ii) using the NeoKinema code v5.4 (Bird & Liu, 2007; Shen & Bird, 2022), a kinematic finite element code that estimates long-term average horizontal velocities at the Earth's surface by weighted least squares fitting of geodetic, geological and geophysical data. It solves an inverse problem, based on a spaced gridded interpolation, with the distance weighted approach (e.g., Cardozo & Allmendinger, 2009), where geological heave rates (i.e., the horizontal component of the net slip) and geodetic velocities are merged to estimate regional tectonic deformation field (i.e., strain rate). Stress directions (Heidbach et al., 2018) are useful to constrain the solution (Bird, 2009; Bird & Carafa, 2016; Bird & Liu, 2007; Carafa & Bird, 2016), but, here, we did not utilize them to obtain our deformation field (see in Supporting Information S1 for details). Other adopted constraints are the use of a refined 5 km mesh grid and the AF-EU Euler vector by Altamimi et al. (2017) (Figure 1). Additional methodological details can be found in the supplementary information and in Bird and Liu (2007), Bird (2009), and Carafa and Bird (2016).

3. Results

The obtained geodetic deformation field with the integration of fault geometries describes the various tectonic settings of southern Italy (Figure 2). We show the strain rate first invariant (2D-dilatation) and second invariant (2nd INV), as defined in Riguzzi et al. (2012) and Kreemer et al. (2014). Three profiles (Figures 2c–2e) are presented to evaluate simulation results from Ionian Sea to South Tyrrhenian Sea, passing through Calabria (section AA', Figure 2d), Messina Strait (section BB', Figure 2e), and Sicily (section CC', Figure 2f). Along those sections, 2D-dilatation and 2nd INV provided by global strain rate model GSRM v2.1 (Kreemer et al., 2014) are also reported for comparison. Grid solution computed with a 5-km spaced resolution, with no smoothing factor, highlights tectonic deformation as obtained in previous studies (Cuffaro et al., 2011; Palano et al., 2012), for example, compression in the southern Tyrrhenian Sea, extension in central Sicily and Calabria, but it also provides a general compression in the Ionian Sea, due to plate motion constraints.

Higher values with respect to those previously computed by Kreemer et al. (2014) are obtained, sometimes exceeding 300 nstrain/a for both 2D-dilatation and 2nd INV estimations (Figure 2). The deformation field in the

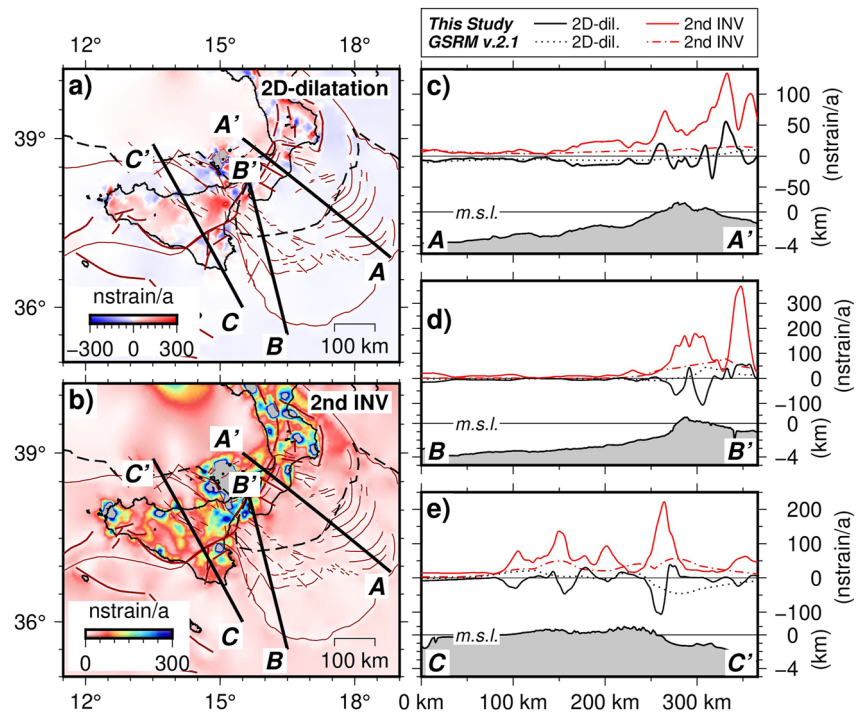


Figure 2. Geodetic strain rate model (this study) for the Southern Tyrrhenian and Ionian Seas. (a) 2D-dilatation and (b) second Invariant with location of the AA', BB', and CC' profiles. Gray areas are those where computed values exceed 300 nstrain/a. Brown lines are the compiled fault lineaments and the dashed black lines are the EU-AF plate boundary from DeMets et al. (2010). (c–e) sections of the AA', BB', and CC' profiles with 2D-dilatation and second Invariant strain rate values and topographic elevation from the Emodnet (<https://emodnet.ec.europa.eu/en/bathymetry>) and the ETOPO 2022 Global Relief Model (www.ncei.noaa.gov/products/etopo-global-relief-model) databases. Along the profiles, a comparison with the GSRM v.2.1 model (Kreemer et al., 2014) is proposed. m.s.l.—mean sea level.

Ionian Sea is like the one by GSRM model v.2.1, but higher and oscillating values are observed onshore Sicily and Calabria (Figure 2).

Predicted fault rakes and net slip rates are obtained and a comparison between observed (OFK) and predicted (PFK) fault kinematics is also provided (Figure 3 and Table S1 in Supporting Information S1). Observed fault kinematics are inferred from literature and the kinematics is assigned to faults according to common rake values for normal ($N = 270 \pm 45$), thrust ($T = 90 \pm 45$), right-lateral ($R = 180 \pm 45$), and left-lateral ($L = 0 \pm 45$) faults (see in Supporting Information S1). Input fault properties are here also used as benchmark to validate the proposed approach and model results, and quantitatively to evaluate model goodness, which is the ratio between the number of PFK concordant with the OFK and the total number of OFK. The computed primary and secondary offset rates for each fault (Table S1 in Supporting Information S1) allowed us to derive net slip (Figure 3).

Overall, 117 predicted fault rakes align with the observed ones over the entire database (Tables S1–S13 in Supporting Information S1), with an obtained ratio of 117/160. The fit is best in the DISS, ELC and WLC sectors, worst in the CSF, COF and SOT ones. Obtained net slip rates are comparable with ones used in input for the DISS sector and, overall, are mostly confined under 0.50 mm/a, except for some other values over 0.80 mm/a, such as 1.37 mm/a for the fault n. 3 (e.g., the Aspromonte-Peloritani seismogenic source, Figures 3a and S2a in Supporting Information S1), or 0.83 and 3.05 mm/a for faults n. 37 and n. 149, respectively (Figures S2b and S5n in Supporting Information S1). Moreover, net slip rate is also evaluated along the two compression fronts of the Drepano and the Apennines systems (Table S14 in Supporting Information S1), providing low values of 0.03 and 0.05 mm/a, respectively.

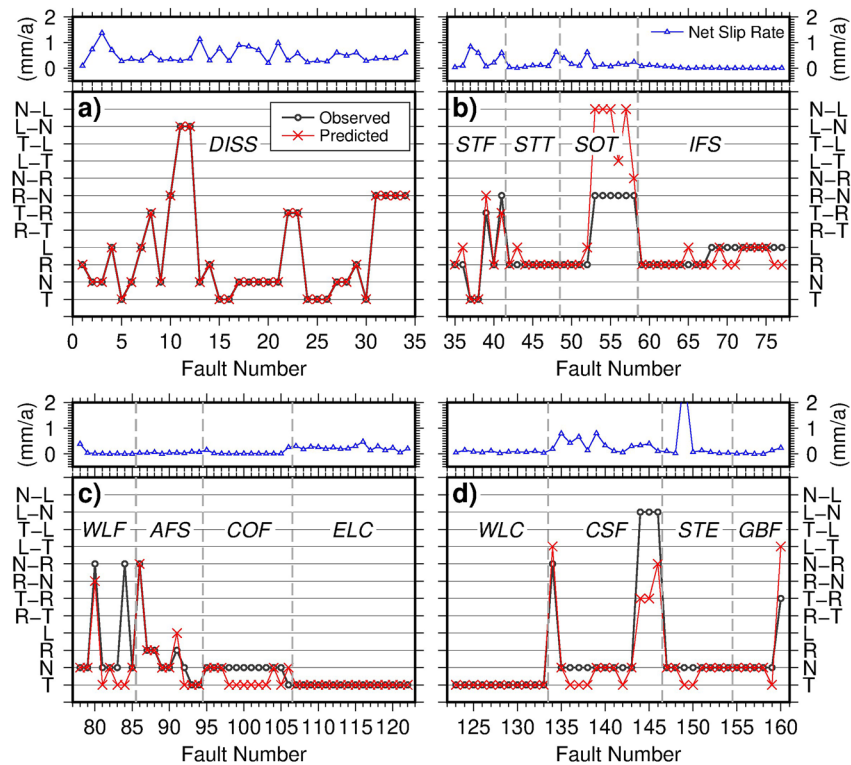


Figure 3. Observed versus predicted fault kinematics for the 160 selected lineaments at different sectors in southern Italy (see text for acronyms). Predicted net slip rate is reported in every upper inset. T–Thrust; N–Normal; R–Right Lateral; L–Left Lateral. As an example, the term N–L represents primary (N) and secondary (L) slip respectively.

4. Discussion and Conclusions

This geodetic/geological integrated approach constitutes a procedure which allowed us to compute the interseismic deformation field in and around southern Italy and obtain the long-term tectonic setting.

We suggest that the higher strain rate values in our model relative to those previously obtained (Billi et al., 2023; Devoti et al., 2011; Kreemer et al., 2014; Palano et al., 2012) are due to the dense network of GNSS stations, the dimension of the computation mesh (from 5 km) and the lack of smoothing function application when the solution grid images are generated (Figure 2). This is observed for closer GNSS stations with variable velocities. For example, it can be verified at the Aeolian Islands or in the region south of the Messina Strait (Figure 2), where the huge number of stations provides a 2D-dilatation and/or second invariant over 300 nstrain/a and a compression south of the Messina Strait, respectively (Figure 2 and Data set S6 in Supporting Information S1). In the former region, the inferred strain is due to the superposition of regional tectonic strain and local strains related to the long-term contraction of a magmatic body at Aeolian Islands (e.g., Cintorrino et al., 2019). In the latter region, compression is also powered by the horizontal component of the imposed initial offset rate for the Aspromonte–Peloritani seismogenic source (fault n. 3, Table S1 in Supporting Information S1).

Since our main purpose is to predict long-term fault kinematics by the integration of space geodesy and geological record, discrepancies with respect to previous strain rate solutions are not discussed here in details. Although strain rate field is not here a primary result, but it contributes to evaluate fault tectonics, it is worth noticing that higher values for geodetic strain rate solutions were previously computed in the Aeolian Island region (Bortoluzzi et al., 2010) and recently proposed by Serpelloni et al. (2022) in northwestern Sicily. A similar strain rate order of magnitude is obtained also using our GNSS solution on a 5 km meshgrid and the SSPX software by Cardozo and Allmendinger (2009) (Figure S10 in Supporting Information S1). Hence, we suggest that the regional signature of our GNSS solution is robust and reliable, providing a detailed snapshot of the ongoing crustal deformation over the study area.

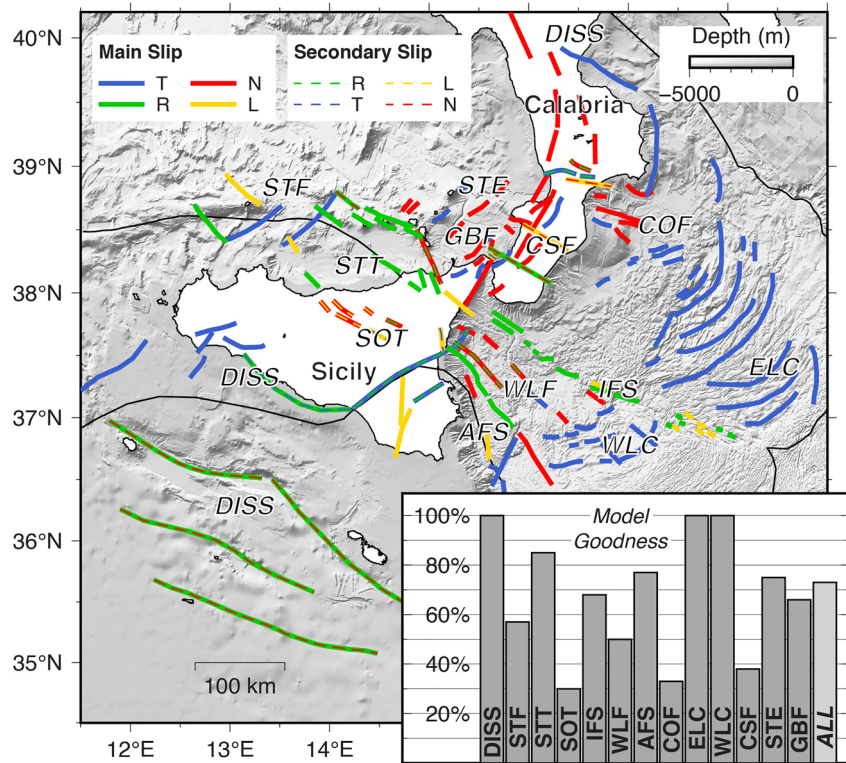


Figure 4. Predicted fault rakes in southern Italy, with primary (solid color) and secondary (dashed color) slip type. Lower right panel shows model goodness, indicating percentage agreement with existing literature (gray bars). See text for acronyms. T–Thrust; N–Normal; R–Right Lateral; L–Left Lateral.

The use of the NeoKinema code also contributes to predict fault kinematics offshore in the South Tyrrhenian Sea, and in the Ionian Sea, because imposed plate motions are used as velocity constraints, when GNSS rates are not available. The estimated uncertainties of primary and secondary slip rates (i.e., the components of the offset rate, Table S1 in Supporting Information S1) are in order of the 10%, and the overall fault kinematic solution describes the behavior of fault displacements in southern Italy (Figure 4), denoting mostly compression in the Ionian Sea, a strike slip displacement with a normal component in the Sicily Channel and a complex kinematics in southern Tyrrhenian Sea, Sicily and Calabria.

Model goodness in the 13 sectors is measured considering the percentage of alignment between predicted and observed fault kinematics (Figure 4). We find an overall agreement with the existing literature in three sectors at 100% (DISS, ELC and WLC), in one over the 80% (STT), and in two over the 70% (AFS and STE). Lower performances are provided in two other sectors over the 60% (IFS and GBF), in two around 50% (STF, and WLF) and in three less than 40% (SOT, COF, and CSF). Overall, the global comparison over the 13 sectors gives an obtained model goodness of 73% (Figure 4).

We suggest that lower performances from onshore sectors can be attributed to the dense number of GNSS stations and by the refined computation meshgrid. Indeed, the SOT and CSF sectors are within the GNSS network (Figure 4), so that we guess that the analyzed faults locally respond to the near deformation field provided by variable GNSS displacements in Sicily and Calabria, lowering the model goodness with respect to the observed fault kinematics derived for instance by Billi et al. (2010), Polonia et al. (2016) and Barreca et al. (2018). The same reasons, but with different percentages, can be proposed for the STF, GBF and STE sectors (Figure 4), where GNSS velocities at Ustica and Aeolian Islands and variable fault directions strongly constrain predicted fault kinematics (Figure 1), or for the case of Capo Peloro Fault (Fault n. 160. Table S13 in Supporting Information S1), where discrepancy between predicted and observed fault kinematics can be attributed to the high number of different GNSS velocity directions in Sicily and Calabria.

Predicted offshore fault kinematics (Figure 4) are mostly constrained by fault location and direction and by far-field kinematic constraints (i.e., GNSS) and mostly by imposed plate motions. This could be the case of the STT, WLF and AFS sectors, where misfit between observed and predicted data can be explained with fault directions with respect to the differences in GNSS velocities between Sicily and Aeolian Islands or Ustica, or relative to the general plate motion directions. Same conclusions can be derived for the IFS sector, where a general right-lateral movement is observed (Polonia et al., 2016), also if in its westernmost part a left-lateral displacement is detected (Gutscher et al., 2017). We suggest that the obtained left-lateral kinematics in the western IFS sector (Figure 4) can be derived by the combination of plate velocity directions and the fault orientation in that domain.

In the COF sector (Figure 4), instead, the extensional kinematics derived by Polonia et al. (2016) and Capozzi et al. (2012) is not aligned with the predicted compression that we obtained, because we suppose that the major constraint due to the imposed convergent AF-EU plate motion at domain boundaries poorly combines with the fault locations and directions in that domain, resulting in overall compression (Figure 4). On the contrary, the distribution of thrusts in the ELC and WLC sectors fully align with the directions of the AF-EU plate motion, resulting in the 100% of model goodness in both the sectors. Finally, the DISS sector (Figure 4) gives a full model goodness also because slip rates are used there as initial constraints, so that the NeoKinema code considers those fault lineaments as active features, when computing the general deformation field coupled with GNSS velocities and imposed plate motions.

Computed net slip rates are in the order of 1 mm/a in average, except for a few higher values (Figure 3) in the DISS sector or in those domains where highly variable GNSS velocity directions are detected (e.g., STF, SOT, CSF, STE); in all the other sectors they are very low, suggesting that the imposed AF-EU plate motion is not capable to provide remarkable computed displacements along fault planes, or emphasizing the major effect of a temporary locking along the AF-EU subduction interface (Carafa et al., 2018).

We remark that the use of the distance weighted approach, the primary and secondary slip uncertainty computation, and the integration of plate kinematics in the resulting deformation field make the NeoKinema code a robust tool to predict tectonic setting and fault kinematics at least in southern Italy. On the contrary, faults are treated as single surfaces, so that with our geometric parameters we cannot investigate parallel structures that converge at depth to one large structure, collecting a larger amount of strain. For this reason, we do not provide considerations on seismic hazard, also if our rake prediction is qualitatively comparable with the focal mechanisms from the European–Mediterranean Regional Centroid-Moment Tensor catalog (Pondrelli, 2002), or from Orecchio et al. (2014), Polonia et al. (2016) and Sgroi et al. (2021), in southern Tyrrhenian and Ionian Seas.

In conclusion, the approach of combining geodetic observation with geological record, using numerical methods, results in computation of a high-resolution deformation field and long-term tectonic setting in a study area, integrating space geodesy, plate motions and fault geometries. The possibility to obtain predicted fault displacements and net slip rates allows us to consider this procedure as a favorable method to improve the knowledge of fault kinematics along diffuse plate boundaries, when faults are known but their kinematic attributes elude us. The procedure level of accuracy can be improved onshore with the increase of GNSS data in a study area, and overall, with a refinement of the angular vectors describing plate motions. Furthermore, the precision increase of fault location onshore and at seafloor is fundamental to avoid artifacts in fault kinematic modeling, and to obtain robust computed crustal deformation fields with the integration of geological constraints.

Data Availability Statement

The source code NeoKinema v.5.4, used to obtain numerical solutions, and the related Guide to Kinematic Modelling of Neotectonics with NeoKinema are provided by Bird (2021). Figures were generated with the Generic Mapping Tools of Wessel et al. (2019). The used models, which describe the input and the output data of this study (e.g., Datasets S1–S6 and Tables S1 and S2 in Supporting Information S1) can be found at Cuffaro et al. (2023).

Acknowledgments

We thank Peter Bird for reading the first version of the manuscript and for sharing the NeoKinema code source. The article was substantially improved by critical comments by Editor Lucy Flesch, Yuanjin Pan and an anonymous reviewer. Edie Miglio is thanked for fruitful discussions. This research was carried out with internal funds at CNR-IGAG and Sapienza Università di Roma.

References

- Allmendinger, R. W., Reilinger, R., & Loveless, J. (2007). Strain and rotation rate from GPS in Tibet, Anatolia, and the Altiplano. *Tectonics*, 26(3). <https://doi.org/10.1029/2006TC002030>
- Allmendinger, R. W., Smalley, J. R., Bevis, M., Caprio, H., & Brooks, B. (2005). Bending the Bolivian orocline in real time. *Geology*, 33(11), 905–908. <https://doi.org/10.1130/G21779.1>
- Altamimi, Z., Métivier, L., Rebischung, P., Rouby, H., & Collilieux, X. (2017). ITRF2014 plate motion model. *Geophysical Journal International*, 209(3), 1906–1912. <https://doi.org/10.1093/gji/ggx136>
- Barreca, G., Corradino, M., Monaco, C., & Pepe, F. (2018). Active tectonics along the south east offshore margin of Mt. Etna: New insights from high-resolution seismic profiles. *Geosciences*, 8(2), 62. <https://doi.org/10.3390/geosciences8020062>
- Billi, A., Cuffaro, M., Orecchio, B., Palano, M., Presti, D., & Toaro, C. (2023). Retracing the Africa-Eurasia nascent convergent boundary in the Western Mediterranean based on earthquake and GNSS data. *Earth and Planetary Science Letters*, 601, 117906. <https://doi.org/10.1016/j.epsl.2022.117906>
- Billi, A., Presti, D., Faccenna, C., Neri, G., & Orecchio, B. (2007). Seismotectonics of the Nubia plate compressive margin in the south Tyrrhenian region, Italy: Clues for subduction inception. *Journal of Geophysical Research*, 112(B8). <https://doi.org/10.1029/2006JB004837>
- Billi, A., Presti, D., Orecchio, B., Faccenna, C., & Neri, G. (2010). Incipient extension along the active convergent margin of Nubia in Sicily, Italy: Cefalù-Etna seismic zone. *Tectonics*, 29(4). <https://doi.org/10.1029/2009TC002559>
- Bird, P. (2003). An updated digital model of plate boundaries. *Geochemistry, Geophysics, Geosystems*, 4(3). <https://doi.org/10.1029/2001GC000252>
- Bird, P. (2009). Long-term fault slip rates, distributed deformation rates, and forecast of seismicity in the western United States from joint fitting of community geologic, geodetic, and stress direction data sets. *Journal of Geophysical Research*, 114(11). <https://doi.org/10.1029/2009JB006317>
- Bird, P. (2021). Kinematic neotectonic modeling with NeoKinema v.5.4 [Software]. <http://peterbird.name/oldFTP/NeoKinema/>
- Bird, P., & Carafa, M. M. C. (2016). Improving deformation models by discounting transient signals in geodetic data: 1. Concept and synthetic examples. *Journal of Geophysical Research: Solid Earth*, 121(7), 5538–5556. <https://doi.org/10.1002/2016JB013056>
- Bird, P., & Liu, Z. (2007). Seismic hazard inferred from tectonics: California. *Seismological Research Letters*, 78(1), 37–48. <https://doi.org/10.1785/gssrl.78.1.37>
- Bortoluzzi, G., Ligi, M., Romagnoli, C., Cocchi, L., Casalbore, D., Sgroi, T., et al. (2010). Interactions between volcanism and tectonics in the western Aeolian sector, southern Tyrrhenian Sea. *Geophysical Journal International*, 183(1), 64–78. <https://doi.org/10.1111/j.1365-246X.2010.04729.x>
- Bortoluzzi, G., Polonia, A., Faccenna, C., Torelli, L., Artoni, A., Carlini, M., et al. (2017). Styles and rates of deformation in the frontal accretionary wedge of the Calabrian Arc (Ionian Sea): Controls exerted by the structure of the lower African plate. *Italian Journal of Geosciences*, 136(3), 347–364. <https://doi.org/10.3301/IJG.2016.11>
- Capozzi, R., Artoni, A., Torelli, L., Lorenzini, S., Oppo, D., Mussoni, P., & Polonia, A. (2012). Neogene to Quaternary tectonics and mud diapirism in the Gulf of Squillace (Crotona-Spartivento Basin, Calabrian Arc, Italy). *Marine and Petroleum Geology*, 35(1), 219–234. <https://doi.org/10.1016/j.marpetgeo.2012.01.007>
- Carafa, M. M. C., & Bird, P. (2016). Improving deformation models by discounting transient signals in geodetic data: 2. Geodetic data, stress directions, and long-term strain rates in Italy. *Journal of Geophysical Research: Solid Earth*, 121(7), 5557–5575. <https://doi.org/10.1002/2016JB013038>
- Carafa, M. M. C., Kastelic, V., Bird, P., Maesano, F. E., & Valensise, G. (2018). A “geodetic gap” in the Calabrian Arc: Evidence for a locked subduction megathrust? *Geophysical Research Letters*, 45(4), 1794–1804. <https://doi.org/10.1002/2017GL076554>
- Cardozo, N., & Allmendinger, R. W. (2009). SSPX: A program to compute strain from displacement/velocity data. *Computers & Geosciences*, 35(6), 1343–1357. <https://doi.org/10.1016/j.cageo.2008.05.008>
- Carminati, E., Lustrino, M., Cuffaro, M., & Doglioni, C. (2010). Tectonics, magmatism and geodynamics of Italy: What we know and what we imagine. *Journal of the Virtual Explorer*, 36, 1–62. <https://doi.org/10.3809/jvirtex.2009.00226>
- Cintorri, A. A., Palano, M., & Viccaro, M. (2019). Magmatic and tectonic sources at Vulcano (Aeolian Islands, Southern Italy): A geodetic model based on two decades of GPS observations. *Journal of Volcanology and Geothermal Research*, 388, 106689. <https://doi.org/10.1016/j.jvolgeores.2019.106689>
- Civile, D., Brancolini, G., Lodolo, E., Forlin, E., Accaino, F., Zecchin, M., & Brancatelli, G. (2021). Morphostructural setting and tectonic evolution of the central part of the Sicilian Channel (Central Mediterranean). *Lithosphere*, 2021, 1–24. <https://doi.org/10.2113/2021/7866771>
- Corti, G., Cuffaro, M., Doglioni, C., Innocenti, F., & Manetti, P. (2006). Coexisting geodynamic processes in the Sicily Channel. In Y. Dilek & S. Pavlides (Eds.), *Post-collisional tectonics and magmatism in the Eastern Mediterranean region* (Vol. 409, pp. 83–95). Geological Society of America Special Paper. [https://doi.org/10.1130/2006.2409\(05\)](https://doi.org/10.1130/2006.2409(05))
- Cuffaro, M., & Doglioni, C. (2018). On the increasing size of the orogens moving from the Alps to the Himalayas in the frame of the net rotation of the lithosphere. *Gondwana Research*, 62, 2–13. <https://doi.org/10.1016/j.gr.2017.09.008>
- Cuffaro, M., Petricca, P., Conti, A., Palano, M., Billi, A., & Bigi, S. (2023). SIFaultKin v.1.1: A dataset of fault kinematic models in Southern Italy (2023). (v.1.1) [Dataset]. Zenodo. <https://doi.org/10.5281/zenodo.10003353>
- Cuffaro, M., Riguzzi, F., Scrocca, D., & Doglioni, C. (2011). Coexisting tectonic settings: The example of the southern Tyrrhenian Sea. *International Journal of Earth Sciences*, 100(8), 1915–1924. <https://doi.org/10.1007/s00531-010-0625-z>
- DeMets, C., Gordon, R. G., & Argus, D. F. (2010). Geologically current plate motions. *Geophysical Journal International*, 181, 1–80. <https://doi.org/10.1111/j.1365-246X.2009.04491.x>
- Devoti, R., Esposito, A., Pietrantonio, G., Pisani, A. R., & Riguzzi, F. (2011). Evidence of large scale deformation patterns from GPS data in the Italian subduction boundary. *Earth and Planetary Science Letters*, 331(3–4), 230–241. <https://doi.org/10.1016/j.epsl.2011.09.034>
- DISS Working Group. (2021). *Database of Individual seismogenic sources (DISS), version 3.3.0: A compilation of potential sources for earthquakes larger than M 5.5 in Italy and surrounding areas*. Istituto Nazionale di Geofisica e Vulcanologia (INGV). <https://doi.org/10.13127/diss3.3.0>
- Doglioni, C., Ligi, M., Scrocca, D., Bigi, S., Bortoluzzi, G., Carminati, E., et al. (2012). The tectonic puzzle of the Messina area (Southern Italy): Insights from new seismic reflection data. *Scientific Reports*, 2(1), 970. <https://doi.org/10.1038/srep00970>
- Gallais, F., Graindorge, D., Gutscher, M. A., & Klaeschen, D. (2013). Propagation of a lithospheric tear fault (STEP) through the western boundary of the Calabrian accretionary wedge offshore eastern Sicily (Southern Italy). *Tectonophysics*, 602, 141–152. <https://doi.org/10.1016/j.tecto.2012.12.026>
- Galli, P., & Peronace, E. (2015). Low slip rates and multimillennial return times for Mw 7 earthquake faults in southern Calabria (Italy). *Geophysical Research Letters*, 42(13), 5258–5265. <https://doi.org/10.1002/2015GL064062>
- Gordon, R. G., & Stein, S. (1992). Global tectonics and space geodesy. *Science*, 256(5055), 333–342. <https://doi.org/10.1126/science.256.5055.333>

- Guillaume, B., Gianni, G. M., Kermarrec, J.-J., & Bock, K. (2022). Control of crustal strength, tectonic inheritance, and stretching/shortening rates on crustal deformation and basin reactivation: Insights from laboratory models. *Solid Earth*, *13*(9), 1393–1414. <https://doi.org/10.5194/se-13-1393-2022>
- Gutscher, M., Dominguez, S., de Lepinay, B. M., Pinheiro, L., Gallais, F., Babonneau, N., et al. (2016). Tectonic expression of an active slab tear from high-resolution seismic and bathymetric data offshore Sicily (Ionian Sea). *Tectonics*, *35*(1), 39–54. <https://doi.org/10.1002/2015TC003898>
- Gutscher, M., Kopp, H., Krastel, S., Bohrmann, G., Garlane, T., Zaragosi, S., et al. (2017). Active tectonics of the Calabrian subduction revealed by new multi-beam bathymetric data and high-resolution seismic profiles in the Ionian Sea (Central Mediterranean). *Earth and Planetary Science Letters*, *461*, 61–72. <https://doi.org/10.1016/j.epsl.2016.12.020>
- Hammond, W. C., Blewitt, G., & Kreemer, C. (2016). GPS Imaging of vertical land motion in California and Nevada: Implications for Sierra Nevada uplift. *Journal of Geophysical Research*, *121*(10), 7681–7703. <https://doi.org/10.1002/2016JB013458>
- Heidbach, O., Rajabi, M., Cui, X., Fuchs, K., Müller, B., Reinecker, J., et al. (2018). The World Stress Map database release 2016: Crustal stress pattern across scales. *Tectonophysics*, *744*, 484–498. <https://doi.org/10.1016/j.tecto.2018.07.007>
- Jiang, Z., Hsu, Y.-J., Yuan, L., Tang, M., Yang, X., & Yang, X. (2022). Hydrological drought characterization based on GNSS imaging of vertical crustal deformation across the contiguous United States. *Science of the Total Environment*, *823*, 823. <https://doi.org/10.1016/j.scitotenv.2022.153663>
- Kreemer, C., Blewitt, G., & Klein, E. C. (2014). A geodetic plate motion and global strain rate model. *Geochemistry, Geophysics, Geosystems*, *15*(10), 3849–3889. <https://doi.org/10.1002/2014GC005407>
- Monaco, C., Bianca, M., Catalano, S., De Guidi, G., & Tortorici, L. (2002). Sudden change in the Late Quaternary tectonic regime in eastern Sicily: Evidences from geological and geomorphological features. *Bollettino della Societa Geologica Italiana*, *1*, 901–913.
- Motaghi, K., Shabanian, E., Tatar, M., Cuffaro, M., & Doglioni, C. (2017). The south Zagros suture zone in teleseismic images. *Tectonophysics*, *694*, 292–301. <https://doi.org/10.1016/j.tecto.2016.11.012>
- Orecchio, B., Presti, D., Totaro, C., & Neri, G. (2014). What earthquakes say concerning residual subduction and STEP dynamics in the Calabrian Arc region, south Italy. *Geophysical Journal International*, *199*(3), 1929–1942. <https://doi.org/10.1093/gji/ggu373>
- Palano, M., Ferranti, L., Monaco, C., Mattia, M., Aloisi, M., Bruno, V., et al. (2012). GPS velocity and strain fields in Sicily and southern Calabria, Italy: Updated geodetic constraints on tectonic block interaction in the central Mediterranean. *Journal of Geophysical Research*, *117*(B7). <https://doi.org/10.1029/2012JB009254>
- Palano, M., Piromallo, C., & Chiarabba, C. (2017). Surface imprint of toroidal flow at retreating slab edges: The first geodetic evidence in the Calabrian subduction system. *Geophysical Research Letters*, *44*(2), 845–853. <https://doi.org/10.1002/2016gl071452>
- Palano, M., Schiavone, D., Loddo, M., Neri, M., Presti, D., Quarto, R., et al. (2015). Active upper crust deformation pattern along the southern edge of the Tyrrhenian subduction zone (NE Sicily): Insights from a multidisciplinary approach. *Tectonophysics*, *657*, 205–218. <https://doi.org/10.1016/j.tecto.2015.07.005>
- Palano, M., Sparacino, F., Gambino, P., D'Agostino, N., & Calcaterra, S. (2022). Slow slip events and flank instability at Mt. Etna volcano (Italy). *Tectonophysics*, *836*, 229414. <https://doi.org/10.1016/j.tecto.2022.229414>
- Palano, M., Ursino, A., Spampinato, S., Sparacino, F., Polonia, A., & Gasperini, L. (2020). Crustal deformation, active tectonics and seismic potential in the Sicily Channel (Central Mediterranean), along the Nubia–Eurasia plate boundary. *Scientific Reports*, *10*(1), 21238. <https://doi.org/10.1038/s41598-020-78063-1>
- Pan, Y., Hammond, W. C., Ding, H., Mallick, R., Jiang, W., Xu, X., et al. (2021). GPS imaging of vertical bedrock displacements: Quantification of two-dimensional vertical crustal deformation in China. *Journal of Geophysical Research*, *126*(4). <https://doi.org/10.1029/2020JB020951>
- Polonia, A., Torelli, L., Artoni, A., Carlini, M., Faccenna, C., Ferranti, L., et al. (2016). The Ionian and Alfeo–Etna fault zones: New segments of an evolving plate boundary in the central Mediterranean Sea? *Tectonophysics*, *675*, 69–90. <https://doi.org/10.1016/j.tecto.2016.03.016>
- Polonia, A., Torelli, L., Gasperini, L., Cocchi, L., Muccini, F., Bonatti, E., et al. (2017). Lower plate serpentine diapirism in the Calabrian Arc subduction complex. *Nature Communications*, *8*(1), 2172. <https://doi.org/10.1038/s41467-017-02273-x>
- Pondrelli, S. (2002). European-mediterranean regional Centroid-Moment Tensors catalog (RCMT) [Dataset]. Istituto Nazionale di Geofisica e Vulcanologia (INGV). <https://doi.org/10.13127/rcmt/euromed>
- Presti, D. (2020). Seismicity supports the theory of incipient rifting in western Ionian sea, central Mediterranean. *Annals of Geophysics*, *62*(Vol 62 (2019)). <https://doi.org/10.4401/ag-8360>
- Proietti, G., Conti, A., Cuffaro, M., Esestima, P., & Bigi, S. (2021). Subduction related faults and sedimentary basins: The Western Ionian Sea case. *Tectonophysics*, *813*, 228943. <https://doi.org/10.1016/j.tecto.2021.228943>
- Riguzzi, F., Crespi, M., Devoti, R., Doglioni, C., Pietrantonio, G., & Pisani, A. R. (2012). Geodetic strain rate and earthquake size: New clues for seismic hazard studies. *Physics of the Earth and Planetary Interiors*, *206–207*, 67–75. <https://doi.org/10.1016/j.pepi.2012.07.005>
- Serpelloni, E., Cavaliere, A., Martelli, L., Pintori, F., Anderlini, L., Borghi, A., et al. (2022). Surface velocities and strain-rates in the Euro-Mediterranean region from massive GPS data processing. *Frontiers in Earth Science*, *10*. <https://doi.org/10.3389/feart.2022.907897>
- Sgroi, T., Polonia, A., Barberi, G., Billi, A., & Gasperini, L. (2021). New seismological data from the Calabrian arc reveal arc-orthogonal extension across the subduction zone. *Scientific Reports*, *473*(1), 473. <https://doi.org/10.1038/s41598-020-79719-8>
- Shen, Z., & Bird, P. (2022). NeoKinema deformation model for the 2023 update to the US National Seismic Hazard Mode. *Seismological Research Letters*, *93*(6), 3037–3052. <https://doi.org/10.1785/0220220179>
- Totaro, C., Orecchio, B., Presti, D., Scolaro, S., & Neri, G. (2016). Seismogenic stress field estimation in the Calabrian Arc region (south Italy) from a Bayesian approach. *Geophysical Research Letters*, *43*(17), 8960–8969. <https://doi.org/10.1002/2016GL070107>
- Wessel, P., Luis, J., Uieda, L., Scharroo, R., Wobbe, F., Smith, W., & Tian, D. (2019). The generic mapping tools version 6. *Geochemistry, Geophysics, Geosystems*, *20*(11), 5556–5564. <https://doi.org/10.1029/2019GC008515>
- Xiao, W., & Santosh, M. (2014). The western Central Asian Orogenic Belt: A window to accretionary orogenesis and continental growth. *Gondwana Research*, *25*(4), 1429–1444. <https://doi.org/10.1016/j.gr.2014.01.008>

References From the Supporting Information

- Aloisi, M., Bruno, V., Cannavò, F., Ferranti, L., Mattia, M., Monaco, C., & Palano, M. (2013). Are the source models of the M 7.1 1908 Messina Straits earthquake reliable? Insights from a novel inversion and a sensitivity analysis of levelling data. *Geophysical Journal International*, *192*(3), 1025–1041. <https://doi.org/10.1093/gji/ggs062>
- Barreca, G., Bruno, V., Cocorullo, C., Cultrera, F., Ferranti, L., Guglielmino, F., et al. (2014). Geodetic and geological evidence of active tectonics in south-western Sicily (Italy). *Journal of Geodynamics*, *82*. <https://doi.org/10.1016/j.jog.2014.03.004>

- Barreca, G., Bruno, V., Cultrera, F., Mattia, M., Monaco, C., & Scarfi, L. (2014). New insights in the geodynamics of the Lipari–Vulcano area (Aeolian Archipelago, southern Italy) from geological, geodetic and seismological data. *Journal of Geodynamics*, 82, 150–167. <https://doi.org/10.1016/j.jog.2014.07.003>
- Barreca, G., Scarfi, L., Cannavo, F., Koulakov, I., & Monaco, C. (2016). New structural and seismological evidence and interpretation of a lithospheric scale shear-zone at the southern edge of the Ionian subduction system (central-eastern Sicily, Italy). *Tectonics*, 35. <https://doi.org/10.1002/2015TC004057>
- Barreca, G., Scarfi, L., Gross, F., Monaco, C., & Guidi, G. D. (2019). Fault pattern and seismotectonic potential at the south-western edge of the Ionian Subduction system (southern Italy): New field and geophysical constraints. *Tectonophysics*, 761, 31–45. <https://doi.org/10.1016/j.tecto.2019.04.020>
- Boncio, P., Mancini, T., Lavecchia, G., & Selvaggi, G. (2007). Seismotectonics of strike-slip earthquakes within the deep crust of southern Italy: Geometry, kinematics, stress field and crustal rheology of the Potenza 1990–1991 seismic sequences (Mmax 5.7). *Tectonophysics*, 445. <https://doi.org/10.1016/j.tecto.2007.08.016>
- Brozzetti, F., Cirillo, D., Liberi, F., Piluso, E., Faraca, E., Nardis, R. D., & Lavecchia, G. (2017). Structural style of Quaternary extension in the Crati Valley (Calabrian Arc): Evidence in support of an east-dipping detachment fault. *Italian Journal of Geosciences*, 136(3), 434–453. <https://doi.org/10.3301/IJG.2017.11>
- Butler, R. (2009). Relationships between the Apennine thrust belt, foredeep and foreland revealed by marine seismic data, offshore Calabria. *Italian Journal of Geosciences*, 128. <https://doi.org/10.3301/IJG.2009.128.2.269>
- Catalano, S., Guidi, G. D., Monaco, C., Tortorici, G., & Tortorici, L. (2008). Active faulting and seismicity along the Siculo–Calabrian Rift Zone (Southern Italy). *Tectonophysics*, 453. <https://doi.org/10.1016/j.tecto.2007.05.008>
- Catalano, S., Romagnoli, G., & Tortorici, G. (2010). Kinematics and dynamics of the Late Quaternary rift-flank deformation in the Hyblean Plateau (SE Sicily). *Tectonophysics*, 486(1–4), 1–s14. <https://doi.org/10.1016/j.tecto.2010.01.013>
- Cinti, F. R., Moro, M., Pantosti, D., Cucci, L., & D'Addezio, G. (2002). New constraints on the seismic history of the Castrovillari fault in the Pollino gap (Calabria, southern Italy). *Journal of Seismology*, 6(2), 199–217. <https://doi.org/10.1023/A:1015693127008>
- Cultrera, F., Barreca, G., Scarfi, L., & Monaco, C. (2015). Fault reactivation by stress pattern reorganization in the Hyblean foreland domain of SE Sicily (Italy) and seismotectonic implications. *Tectonophysics*, 661, 215–228. <https://doi.org/10.1016/j.tecto.2015.08.043>
- D'Agostino, N., & Selvaggi, G. (2004). Crustal motion along the Eurasia–Nubia plate boundary in the Calabrian Arc and Sicily and active extension in the Messina Straits from GPS measurements. *Journal of Geophysical Research*, 109(B11). <https://doi.org/10.1029/2004JB002998>
- Di Bucci, D., Ravaglia, A., Seno, S., Toscani, G., Fracassi, U., & Valensise, G. (2006). Seismotectonics of the Southern Apennines and Adriatic foreland: Insights on active regional E–W shear zones from analogue modeling. *Tectonics*, 25. <https://doi.org/10.1029/2005TC001898>
- Fabbi, A., Ghisetti, F., & Vezzani, L. (1980). The Peloritani–Calabria range and the Gioia basin in the Calabrian Arc (Southern Italy): Relationships between land and marine data. *Geologica Romana*, 19, 131–150.
- Ferranti, L., Burrato, P., Pepe, F., Santoro, E., Mazzella, M. E., Morelli, D., et al. (2014). An active oblique-contractional belt at the transition between the Southern Apennines and Calabrian Arc: The Amendolara Ridge, Ionian Sea, Italy. *Tectonics*, 33(11), 2169–2194. <https://doi.org/10.1002/2014TC003624>
- Ferranti, L., Pepe, F., Barreca, G., Meccariello, M., & Monaco, C. (2019). Multi-temporal tectonic evolution of Capo Granitola and Sciacca foreland transcurent faults (Sicily channel). *Tectonophysics*, 765, 187–204. <https://doi.org/10.1016/j.tecto.2019.05.002>
- Ferranti, L., Monaco, C., Morelli, D., Antonielli, F., & Maschio, L. (2008). Holocene activity of the Scilla Fault, Southern Calabria: Insights from coastal morphological and structural investigations. *Tectonophysics*, 453(1–4), 74–93. <https://doi.org/10.1016/j.tecto.2007.05.006>
- Gallais, F., Gutscher, M. A., Graindorge, D., & Klaeschen, D. (2012). Two-stage growth of the Calabrian accretionary wedge in the Ionian Sea (Central Mediterranean): Constraints from depth migrated multichannel seismic data. *Marine Geology*, 326, 28–45. <https://doi.org/10.1016/j.margeo.2012.08.006>
- Galli, P., & Bosi, V. (2003). Catastrophic 1638 earthquakes in Calabria (southern Italy): New insights from paleoseismological investigation. *Journal of Geophysical Research*, 108(B1). <https://doi.org/10.1029/2001JB001713>
- Galli, P., & Peronace, E. (2014). New paleoseismic data from the Irpinia Fault. A different seismogenic perspective for southern Apennines (Italy). *Earth-Science Reviews*, 136, 175–201. <https://doi.org/10.1016/j.earscirev.2014.05.013>
- Galli, P., & Scionti, V. (2006). Two unknown M > 6 historical earthquakes revealed by paleoseismological and archival researches in eastern Calabria (southern Italy). Seismotectonic implication. *Terra Nova*, 18. <https://doi.org/10.1111/j.1365-3121.2005.00658.x>
- Loreto, M. F., Fracassi, U., Franzo, A., Negro, P. D., Zgur, F., & Facchin, L. (2013). Approaching the seismogenic source of the Calabria 8 September 1905 earthquake: New geophysical, geological and biochemical data from the S. Eufemia Gulf (S Italy). *Marine Geology*, 343. <https://doi.org/10.1016/j.margeo.2013.06.016>
- Loreto, M. F., Pepe, F., De Ritis, R., Ventura, G., Ferrante, V., Speranza, F., et al. (2015). Geophysical investigation of Pleistocene volcanism and tectonics offshore Capo Vaticano (Calabria, southeastern Tyrrhenian Sea). *Journal of Geodynamics*, 99, 71–86. <https://doi.org/10.1016/j.jog.2015.07.005>
- Maschio, L., Ferranti, L., & Burrato, P. (2005). Active extension in Val d'Agri area, Southern Apennines, Italy: Implications for the geometry of the seismogenic belt. *Geophysical Journal International*, 162(2), 591–609. <https://doi.org/10.1111/j.1365-246X.2005.02597.x>
- Michetti, A. M., Ferrel, L., Esposito, E., Porfido, S., Blumetti, A. M., Vittori, E., et al. (2000). Ground effects during the 9 September 1998, Mw=5.6, Lauria earthquake and the seismic potential of the “aseismic” Pollino region in southern Italy. *Seismological Research Letters*, 71(1), 31–46. <https://doi.org/10.1785/gssrl.71.1.31>
- Monaco, C., & Tortorici, L. (2000). Active faulting in the Calabrian arc and eastern Sicily. *Journal of Geodynamics*, 29(3–5), 407–424. [https://doi.org/10.1016/S0264-3707\(99\)00052-6](https://doi.org/10.1016/S0264-3707(99)00052-6)
- Musumeci, C., Scarfi, L., Palano, M., & Patanè, D. (2014). Foreland segmentation along an active convergent margin: New constraints in southeastern Sicily (Italy) from seismic and geodetic observations. *Tectonophysics*, 630, 137–149. <https://doi.org/10.1016/j.tecto.2014.05.017>
- Pepe, F., Bertotti, G., Ferranti, L., Sacchi, M., Collura, A., Passaro, S., & Sulli, A. (2014). Pattern and rate of post-20 ka vertical tectonic motion around the Capo Vaticano Promontory (W Calabria, Italy) based on offshore geomorphological indicators. *Quaternary International*, 332, 85–98. <https://doi.org/10.1016/j.quaint.2013.11.012>
- Pepe, F., Sulli, A., Bertotti, G., & Catalano, R. (2005). Structural highs formation and their relationship to sedimentary basins in the north Sicily continental margin (southern Tyrrhenian Sea): Implication for the Drepano Thrust Front. *Tectonophysics*, 409(1–4), 1–18. <https://doi.org/10.1016/j.tecto.2005.05.009>
- Presti, D., Billi, A., Orecchio, B., Totaro, C., Faccenna, C., & Ner, G. (2013). Earthquake focal mechanisms, seismogenic stress, and seismotectonics of the Calabrian Arc, Italy. *Tectonophysics*, 602, 153–175. <https://doi.org/10.1016/j.tecto.2013.01.030>
- Roda-Boluda, D. C., & Whittaker, A. C. (2017). Structural and geomorphological constraints on active normal faulting and landscape evolution in Calabria, Italy. *Journal of the Geological Society*, 174(4), 701–720. <https://doi.org/10.1144/jgs2016-097>

- Scarfi, L., Barberi, G., Musumeci, C., & Patanè, D. (2016). Seismotectonics of northeastern Sicily and southern Calabria (Italy): New constraints on the tectonic structures featuring in a crucial sector for the central Mediterranean geodynamics. *Tectonics*, 35(3), 812–832. <https://doi.org/10.1002/2015TC004022>
- Serpelloni, E., Vannucci, G., Pondrelli, S., Argnani, A., Casula, G., Anzidei, M., et al. (2007). Kinematics of the Western Africa-Eurasia plate boundary from focal mechanisms and GPS data. *Geophysical Journal International*, 169(3), 1180–1200. <https://doi.org/10.1111/j.1365-246X.2007.03367.x>
- Sgroi, T., de Nardis, R., & Lavecchia, G. (2012). Crustal structure and seismotectonics of central Sicily (southern Italy): New constraints from instrumental seismicity. *Geophysical Journal International*, 189(3), 1237–1252. <https://doi.org/10.1111/j.1365-246X.2012.05392.x>
- Tansi, C., Muto, F., Critelli, S., & Iovine, G. (2007). Neogene-Quaternary strike-slip tectonics in the central Calabrian Arc (southern Italy). *Journal of Geodynamics*, 43(3), 393–414. <https://doi.org/10.1016/j.jog.2006.10.006>
- Tondi, E., Zampieri, D., RendaAlessandriniUnti, G. G. P. M., Giorgianni, A., & Cello, G. (2006). Active faults and inferred seismic sources in the San Vito Lo Capo peninsula, northwestern Sicily, Italy. In G. Moratti & A. Chalouan (Eds.), *Tectonics of the Western Mediterranean and North Africa* (Vol. 262, pp. 365–377). Geological Society, London, Special Publication. <https://doi.org/10.1144/GSL.SP.2006.262.01.22>
- Twiss, R., & Moores, E. (1992). *Structural geology*. W.H. Freeman and Company.